Analysis of a heat exchanging asphalt layer using a finite element approach

Cedric Vuye[1, a], Gert Guldentops[2, b], Nima Rahbar[2], Alireza Mahdavi Nejad[2], Wim Van den bergh[1, c]

[1] *Faculty of Applied Engineering, University of Antwerp, Antwerp, Belgium*
[2] *Civil and Environmental Engineering, Worcester Polytechnic Institute, Worcester, United States*

[a] cedric.vuye@uantwerpen.be
[b] gguldentops@wpi.edu
[c] wim.vandenbergh@uantwerpen.be

Digital Object Identifier (DOI): dx.doi.org/10.14311/EE.2016.361

ABSTRACT

Current aims regarding environmental protection, like reduction of fossil fuel consumption and greenhouse gas emissions, require the development of new technologies. These new technologies should enable the production of renewable energy which is both cleaner and cheaper. This necessity encourages engineers to develop new ways to capture energy for later use. In this paper, the use of a heat exchanging asphalt layer (HEAL), as a means to extract low temperature heat, is studied in detail. Such a system, which harvests heat energy by flowing water through a heat exchanger embedded in the pavement structure, could definitely have a significant thermal energy output since pavement materials absorb large amounts of solar insolation.
The focus in this paper is on asphalt concrete pavements since these absorb the largest amount of solar insolation and will benefit the most from the removal of heat in the form of an increase in lifetime. The main objective is to study the energy output and efficiency of the HEAL. In order to achieve this, a parametric study on different thermal properties of the asphalt pavement has been performed using a validated Finite Element (FE) model of the collector. It is shown that both the absorptivity and thermal conductivity have a large influence on the outlet temperature and solar efficiency. Using this FE model it will be possible to predict the long-term energy output of the HEAL taking into account all geometrical, material and weather parameters.

Keywords: Climate change, De-icing, Energy saving

1. INTRODUCTION

Asphalt Concrete (AC) road surfaces absorb significant amounts of solar radiation on a daily basis, up to 40 MJ/m² over the course of a day during summer, which causes high temperatures in the pavement structure.[1] This heat energy can be harvested using a heat exchanger system embedded in the pavement structure [2]-[4]. An operating fluid flows through the heat exchanger, thus, cooling down the pavement by extracting energy. This not only reduces the potential Urban Heat Island (UHI) effect [3], rutting damage and fatigue due to oxidation of the binder [4], but also provides heat energy which could potentially be used for different purposes. Heat Exchanging Asphalt Layers (HEAL) have a lower efficiency compared to the classic solar collector panels, but also the materials used in a pavement collector are lower in cost. Also, pavement surfaces are widely available and can still be used for other purposes, like a car park.
Since AC has a much larger absorptivity regarding solar radiation compared to other pavement materials, it is reasonable to assume that AC solar collectors have a larger efficiency and output compared to, for example, a cement concrete solar collector.[5]
HEAL systems are an appealing candidate in extracting thermal energy from pavements or de-icing systems. Recently, there have been some experimental and modelling efforts of these systems by some research groups [6]-[10]. Recently, the performance and parametric analysis of air-powered energy harvesting pavements have been discussed in [11]. However, it remains difficult to predict the total energy output of a large scale HEAL system. Hence, it is difficult to determine the feasibility of the system and its overall performance. Consequently, it is arduous to predict the applicability of the harvested low temperature heat energy.
In this paper, in order to fill this knowledge gap, a modelling framework is developed, and verified experimentally, that can predict the heat energy output of a complete HEAL system with a high degree of accuracy. Such a framework will help us to determine potential design strategies on how to improve such a system. In Section 2 of this paper, the underlying FE model of the HEAL is presented. An experiment has been carried out to validate the numerical results, which is discussed in Section 3. A preliminary parametric study on two of the most important thermal properties is conducted in Section 4. The paper is then finalized with a discussion and general conclusions in Section 5.

2. FINITE ELEMENT MODEL

First of all an overview of the governing equations and boundary conditions (BC) is given before the Finite Element (FE) model itself is discussed.

2.1 Pavement surface BC equation

At the surface of the asphalt pavement, seven different heat transfer modes and sub-modes take place, including conduction, absorption and reflection of solar radiation, absorption and reflection of longwave radiation, emission of longwave radiation, and convection. Each of these mechanisms were considered in the BC equation for the surface of the pavement structure (see Eq. 1) [12]–[15].

$$-\lambda T_{i,j} = \alpha_{sw}\, q''_{sw} + \varepsilon\sigma\left(T_{sky}^4 - T^4\right) + h(T_a - T) \qquad \text{(Eq. 1)}$$

α_{sw} is the shortwave (solar) radiation absorption coefficient, or solar absorptivity, and q''_{sw} is the specific incident solar radiation heat flux. In the longwave radiation part of Eq. 1, more specifically $\varepsilon\sigma\left(T_{sky,i}^4 - T^4\right)$, the Stefan-Boltzmann law ($E_b = \sigma T^4$) was used to calculate the net amount of longwave radiation exchanged between the pavement and its surroundings in combination with the following assumptions: (i) emissivity equals the spectral absorptivity, and (ii) grey surface behaviour. The latter is the assumption that the spectral absorptivity and emissivity are independent of wavelength [16]. Here, ε denotes the emissivity of the pavement, whilst T_{sky} denotes the hypothetical temperature of the surroundings that is used to estimate the temperature of the surrounding atmosphere, which absorbs and emits radiation. It can be calculated using the Bliss model (Eq. 2) [5]-[6]. The convection coefficient, h, will be derived

using Eq. 4, which is discussed further. Finally, T_a denotes the dry-bulb air temperature as measured by a standardized weather station.

$$T_{sky} = \left(0.8 + \frac{T_{dp}}{250}\right)^{0.25} T_a \qquad \text{(Eq. 2)}$$

In Eq. 2, T_{dp} is the dew point temperature. The dew point temperature can be calculated with a high accuracy using the following Eq. 3, which is based on the dry-bulb air temperature and relative humidity (RH) [17].

$$T_{dp} = \frac{B\left[log\left(\frac{RH}{100}\right) + \frac{C\,T_a}{B+T_a}\right]}{C - log\left(\frac{RH}{100}\right) - \frac{C\,T_a}{B+T_a}} \qquad with\ B = 243.04\ and\ C = 17.625 \qquad \text{(Eq. 3)}$$

The empirical Bentz model was employed to estimate the heat transfer coefficient, h, to characterize the thermal boundary layer just above the pavement's surface regarding heat transfer due to convection [15]. This model only uses the wind velocity (v) as an input factor, although it does give the best result out of most common empirical models developed for calculating the heat transfer coefficient [5].

$$\begin{aligned} &If\ v \leq 5\,m/s \qquad h = 5.6 + 4.0\,v \\ &If\ v > 5\,m/s \qquad h = 7.2\,v \end{aligned} \qquad \text{(Eq. 4)}$$

All values of T_{sky}, T_{dp}, and h are updated using Eqs. 2-4 at the beginning of each time step in the simulation. Values of q''_{sw}, T_a, RH, and v need to be updated based on hourly values provided by given tables from various meteorological databases such as in the *Meteonorm* software.

The HEAL ceases its operation during the night due to the lack of incident solar radiation and the subsequent drop in pavement temperatures. This inactivity transforms the thermal state of the HEAL overnight towards a state with a one dimensional temperature profile. This temperature profile can be estimated with reasonable accuracy using a simple set of empirical equations (Eqs. 5-6) [2] often used for predicting the temperature profile of regular pavement structures containing asphalt concrete. This functions as the initial temperature field for the modelling framework developed here.

$$T_{s,sunrise} \cong T_{s,min} = 0.89\,T_{a,min} + 5.2 \qquad \text{(Eq. 5)}$$

$$T_{pavement} = T_{s,min} + (0.037\ depth) - (6.29 \cdot 10^{-5}\ depth^2) \qquad \text{(Eq. 6)}$$

Just before sunrise, the daily minimum pavement surface temperature ($T_{s,min}$) tends to be reached, and it can be estimated as a function of the daily minimum dry-bulb air temperature ($T_{a,min}$) (Eq. 5), which tends to occur around the same time. With a similar empirical formula, Eq. 6, the temperature profile of the pavement structure can be further estimated based on the previously calculated minimum surface temperature and as a function of depth. In Eq. 6, $depth$ is the distance, expressed in mm, between the pavement surface and the point of interest perpendicular to the pavement surface [2].

An adiabatic boundary ($\frac{\partial T}{\partial n} = 0$) is assumed at a depth of 300 mm. This assumption is safe since past observations indicate minimal to no temperature variations over the course of the simulated time frames, which never exceeded 24 hours [5].

2.2 Governing equations and BC equations

The governing equations in the system are incompressible Navier-Stokes equations:

$$\rho\nabla(\boldsymbol{u}) = 0 \qquad \text{(Eq. 7)}$$

$$\rho(\boldsymbol{u}\cdot\nabla)\boldsymbol{u} = \nabla[-p + \mu\nabla\boldsymbol{u}] \qquad \text{(Eq. 8)}$$

with **u** and p denoting the velocity vector and pressure, respectively. μ is working fluid dynamic viscosity, whilst ρ is working fluid density.
The flow was computed with the boundary conditions in two consecutive steps. First, a uniform velocity BC ($u_i = -U_0$) and far field pressure ($p = p_\infty$) were prescribed for pipe inlet and outlet, respectively. Then, to achieve a fully developed flow in the system, the outlet velocity profile in step 1 is set for pipe inlet, $u_i = u(x, y)$. The pipe wall had a no-slip velocity BC, $u_{wall} = 0$. In the laminar flow solver, the working fluid is assumed to be pure water at a temperature of 20°C. Therefore, all properties of the working fluid were assumed at 20°C, which is a reasonable assumption for a laminar flow. High-end and low-end working fluid properties have been simulated in order to verify the negligible influence of variable viscosity and density. This is done for the case of pure water. No other working fluids were assumed during the simulations.

The transient heat transfer problem has Eq. 9 as its governing equation, which is the general energy equation. To solve this equation the flow field of the stationary solver is employed during each time step.

$$\rho c_p \left[\frac{\partial T}{\partial t} + (\boldsymbol{u} \cdot \nabla)T\right] = \nabla(\lambda \nabla T) + (\bar{\bar{\tau}} \cdot \nabla)\boldsymbol{u} \qquad \text{(Eq. 9)}$$

with T temperature, t time, λ thermal conductivity, and c_p specific isobaric thermal capacity. $\bar{\bar{\tau}}$ represents the stress tensor due to viscous shear.
Constant temperature was assumed at fluid inlet ($T_{inlet} = T_0$). The pipe wall also holds a no-slip temperature BC ($T_{wall} = T_{fluid}$). In the transient heat transfer solver, the properties of the working fluid are assumed to be temperature dependent during the heat transfer simulation, although this does not have a major effect on the results.

2.3 Pavement materials and properties

All pavement materials are heterogeneous and exhibit a large number of internal heat transport mechanisms. Because of this, it is necessary to simplify the way the thermal properties are defined. Here, it is assumed that the pavement materials behave as a homogenous material with isotropic thermal properties. Table 1 contains all the thermal properties that were used in this work. It has been previously shown that asphalt concrete has a thermal conductivity between 0.75 and 2.89 W/(m.K) [18]. Significant variations in thermal properties of the aggregates cause large differences in the thermal conductivity of the asphalt concrete [9]. However, very often, the reference material tends to report values between 0.8 and 1.5 W/(m.K) [19]. The thermal properties of the pipes and pavement materials are assumed to be temperature independent.

Table 1: Thermal properties of pavement materials.

Material	α	λ [W/m.K]	c_p [J/kg.K]	ρ [kg/m³]
Reference AC	0.9	1.2	950	2350
Crushed gravel [5]	N.A.	1.1	1000	2200
Dry soil [19]	N.A.	1.0	1900	1500
Concrete foundation [5]	N.A.	2.3	1050	2300

2.4 Model development

In this study, the geometry of the HEAL consists of a number of horizontal pavement layers, one of which contains at least one pipe loop that acts as a heat exchanger. The entire HEAL is modelled in 3D using the finite element method, during which thin wall assumptions or other geometric simplifications are not applied. This approach allows for a comprehensive evaluation of the system. Accurate models are necessary for the future development of the HEAL system.
The pipe is always laid out in a serpentine fashion, which should give the highest possible outlet temperature and is the most pragmatic to construct. Only the top 300 mm of pavement structure was modeled, as explained in the following section. Each pipe

loop is assumed to behave independently within the HEAL structure. Hence, the equations are solved for only one loop. Geometrical parameters which characterize the design of the HEAL are specified as follows: horizontal distance between two parallel pipe lengths, P, inner diameter of the pipe, D_{in}, outer diameter of the pipe, D_{out}, the depth of pipe burial, P_d, which denotes the distance between the pavement surface and the upper level of the pipe, total length of the HEAL area, L, thickness of each individual pavement layer, d_i, and properties of materials in the system. The width, W, and total area of the HEAL can be calculated as a function of the above parameters. Figure 1 shows all geometric parameters involved in this study.

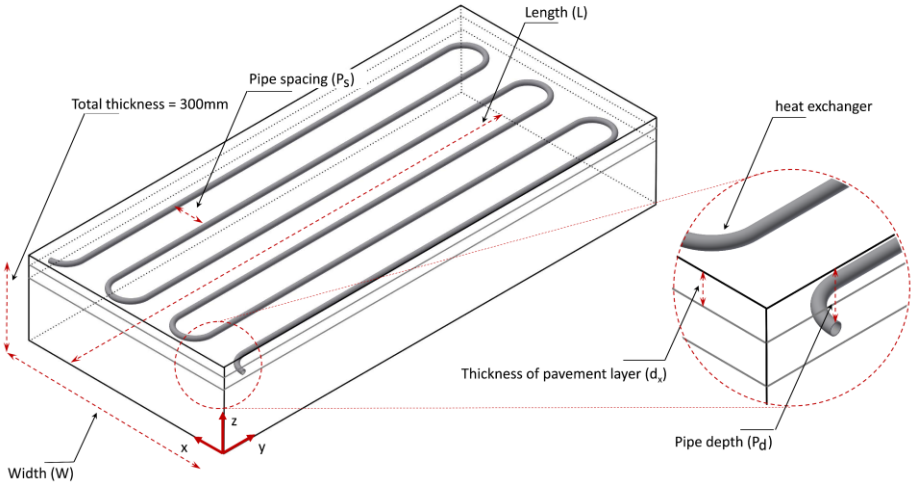

Figure 1: Schematic of involved geometric parameters in the HEAL system.

It is assumed that the flow problem is uncoupled from the thermal problem, which is a reasonable assumption in the case of a laminar flow. This allows us to split the problem into two separate problems, and employ two consecutive solvers. The first problem is approached using a laminar flow solver for a stationary case, and the second problem involves solving the transient temperature in the entire HEAL system. This approach is computationally economical due to only having to solve for one flow field. The only drawback is the non-variability of the flow rate during system operation. The software used to develop this model was COMSOL Multiphysics.

The mesh of the FEM is a combination of prismatic elements with a triangular base (for the middle part of the model), and tetrahedral elements for the end parts of the collector geometry. Larger elements were used parallel to the fluid flow and much smaller elements were necessary perpendicular to the fluid flow. The smallest elements were used in and around the heat exchanger pipes.

The system is meshed using tetrahedral and prismatic elements, as can be seen in Figure 2. A minimum of 200,000 elements was needed for a HEAL measuring 1 m². A detailed grid study has been performed to determine the maximum element size in different parts of the geometry.

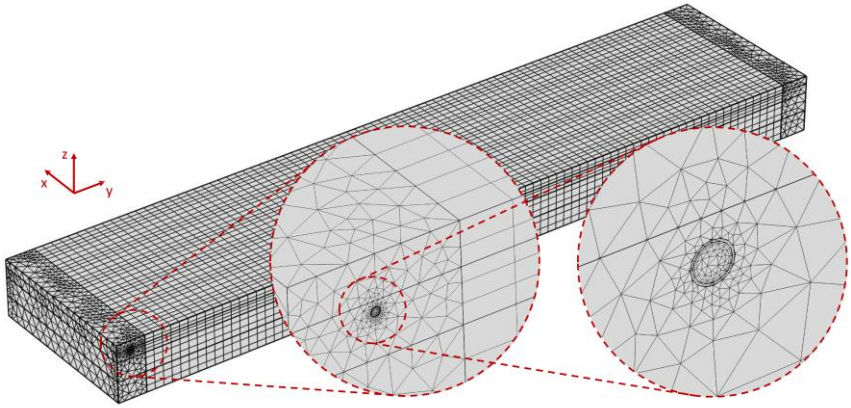

Figure 2: Mesh of the model with L = 4 m, W = 0.9 m and total pipe length 24 m.

3. FE MODEL VALIDATION

To validate the FE model the predicted temperatures are compared to actual thermocouple measurements on a small scale prototype. The first part of this Section is dedicated to the description of the prototype while the second part deals with the actual comparison.

3.1 Prototype

The experimental prototype consists of a slab of AC (3' by 6', approx.. 0.9 by 1.8 m) with embedded copper pipes. The slab had a total thickness of 4.7" (119 mm). Two types of AC were used to make the slab. The bottom 2.5" (64 mm) of the slab was prepared with a local mix of AC obtained from an asphalt plant. In the top layer an AC with quartzite aggregates, prepared in the laboratory, was used. The thermal properties of these asphalt mixes are depicted in Table 2 [9].

Table 2: Material properties in prototype.

Material	λ [W/m.K]	c_p [J/kg.K]	ρ [kg/m³]
Laboratory AC	1.8	950	2350
Commercial AC	1.0	1050	2350
Copper	400	1900	8700

Figure 3 shows the schematic design and the actual laboratory prototype.

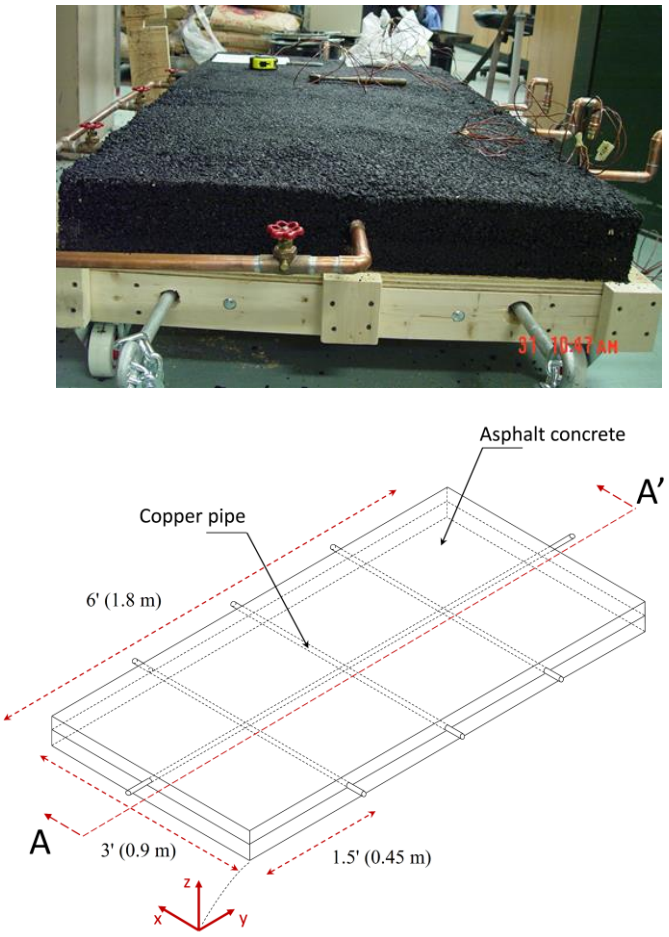

Figure 3: Overview of the laboratory prototype.

Cross section AA' is shown in Figure 4 to give an overview of the thermocouple locations. The asphalt temperature was measured at multiple locations in the slab in both the X- and Y-direction. The outlet fluid temperature was measured using a submergible thermocouple (n° 14 in Figure 4).

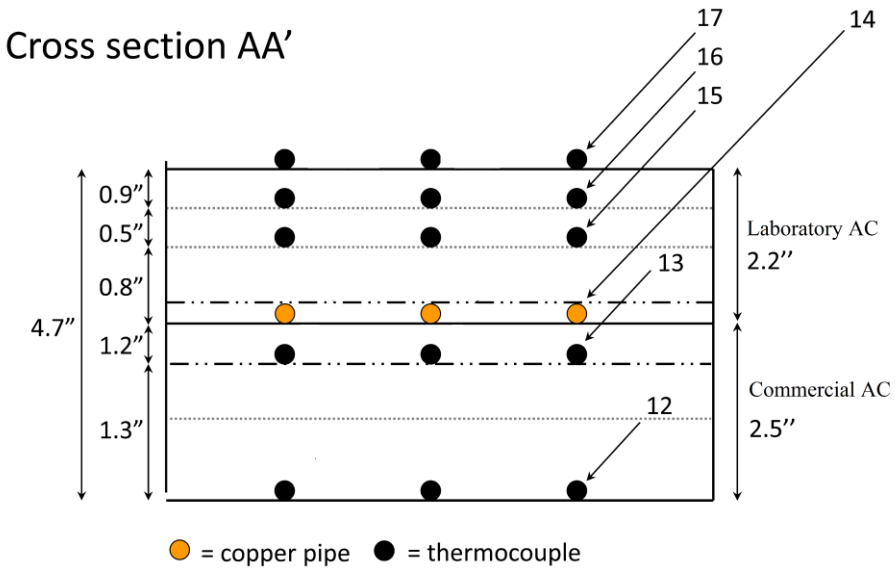

Figure 4: Locations of the thermocouples.

The asphalt slab was placed outside for the actual measurements. The incident solar radiation was measured using a Kipp & Zonen/Campbell Scientific CMP-3 pyranometer while the wind velocity was monitored using a Campbell Scientific 014A-L anemometer. The air temperature was measured using a shaded thermocouple. The incident solar radiation and air temperature reached a maximum of 785 W/m² and 34.3°C, respectively. The wind velocity fluctuated between 0 and 2 m/s. These measured weather parameters were used in the FE model as well.
The experiment itself consisted of the following steps:

1) 4 hours in the sun without water flowing
2) Flow rates changing from 1 to 4 l/min in steps of 1 l/min

The inlet temperature was measured four times during the experiment and ranged between 22 and 24 °C.

3.2 Comparison

Thermocouple T14 (see cross section in Figure 4) recorded the outlet temperature in one point of the pipe outlet cross section. Two values, maximum and minimum outlet temperatures, were obtained for each time step from the FE model in order to be compared with the experimental results, see Figure 5. Due to the small inner pipe diameter and a fully developed flow assumption, it was expected that the outlet temperature would plot in the same range. However, due to the random movement of the thermocouple, the registered point is not exactly fixed over the time and can, therefore, be assumed anywhere over the cross section of the outlet. The experimental data is located in between the maximum and minimum simulated outlet temperature data. As the experimental data is closer to the computed maximum temperature, which occurs at the inner pipe wall surface, it is reasonable to assume that the thermocouple was located somewhere in the vicinity of the pipe wall. Therefore, it can be observed that there is a good agreement on outlet temperature between the model and the experiment.

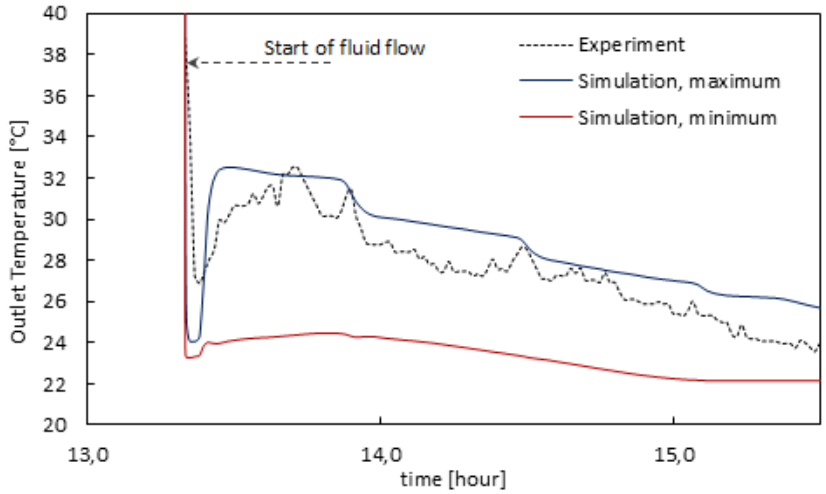

Figure 5: Outlet temperatures measured (T14) and predicted by FE Model

It can also be observed from Figure 6 that the temperature measurements from the thermocouples, embedded within the asphalt concrete of the experimental set-up, follow the same trend as their simulated counterparts. The surface temperature (T17) during the experiment and simulation lie closely together, except for the maximum surface temperature, which was predicted to be slightly higher from the simulation. The thermocouples located between the surface of the asphalt concrete and the copper pipe recorded higher temperatures during the experiment compared to the FE simulation, although with a similar trend. This difference can simply be explained by the empirical nature of Eqs. 8 and 9 which calculate a rough estimate for the initial temperature of the HEAL slab. Uncertainties in the thermal properties of the material and the exact location of the thermocouples are also contributing factors. However, the comparison between the experimental data and the simulation results clearly verifies the modelling framework.

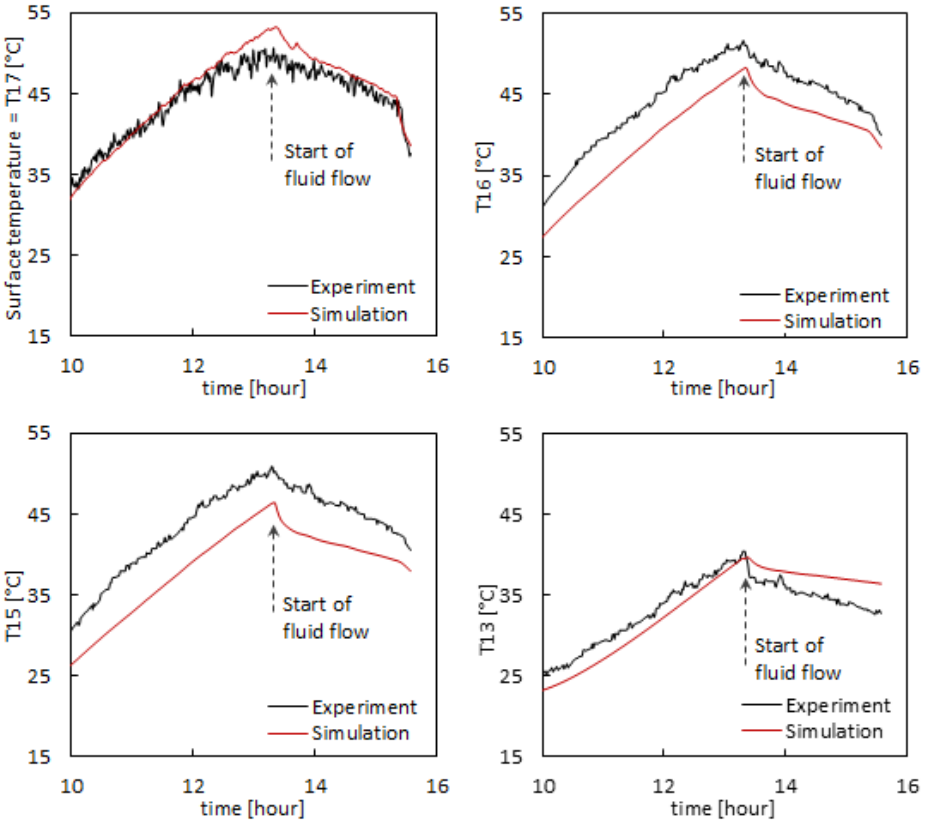

Figure 6: Comparison of measured and predicted asphalt temperatures

4. PRELIMINARY PARAMETRIC STUDY

A preliminary parametric study on both the thermal conductivity and the solar absorption coefficient of the asphalt concrete is performed, using the FE model developed above. The weather input parameters are based on real weather data from Albuquerque, New Mexico (US). A pipe spacing of 150 mm, a pipe depth of 55 mm and an inside diameter of 8 mm were used for the following simulations. The inlet water temperature was kept constant at 15°C with a flow rate of 50 l/hr. A surface of 4 m by 2.7 m (10.8 m² and 70 m of heat exchanger) was simulated during a complete day. For the asphalt concrete (90 mm in total with 250 mm crushed gravel as the foundation) the solar absorption and thermal conductivity were chosen as 0.9 and 2.0 W/mK respectively, unless they were changed in the parametric study. Figure 7 shows a cross section of one of the performed simulations. The inlet water temperature can be found on the left and the outlet temperature on the right.

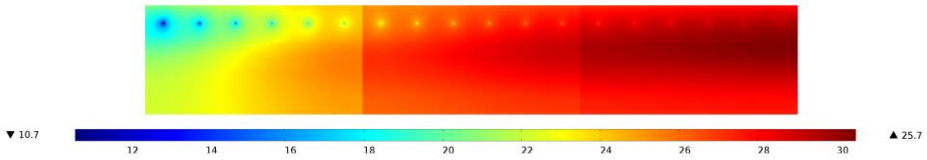

Figure 7: Cross section of a COMSOL simulation.

The efficiency of the collector (η_{solar}) is defined as the ratio between energy outputs achieved with the HEAL (Q_{HEAL}) and the thermal energy of the incident solar radiation (Q_{sw}).

A higher thermal conductivity results in a sharper increase in working fluid temperature over the length of the heat exchanger pipe, leading to a higher outlet temperature (37°C with λ = 1 W/mK up to 42°C with λ = 2.5 W/mK), see Figure 8, and higher peak asphalt temperatures. As both the outlet temperature and solar efficiency seem to taper off at higher λ, increasing the thermal conductivity further would be of little consequence to the outlet temperature and efficiency of the HEAL.
An increase of λ can compensate for a shorter heat exchanger or a smaller surface. In this simulation the same outlet temperature, with 70 m of pipes and λ = 1 W/mK, can be obtained with only 36 m when λ is increased to 2 W/mK.

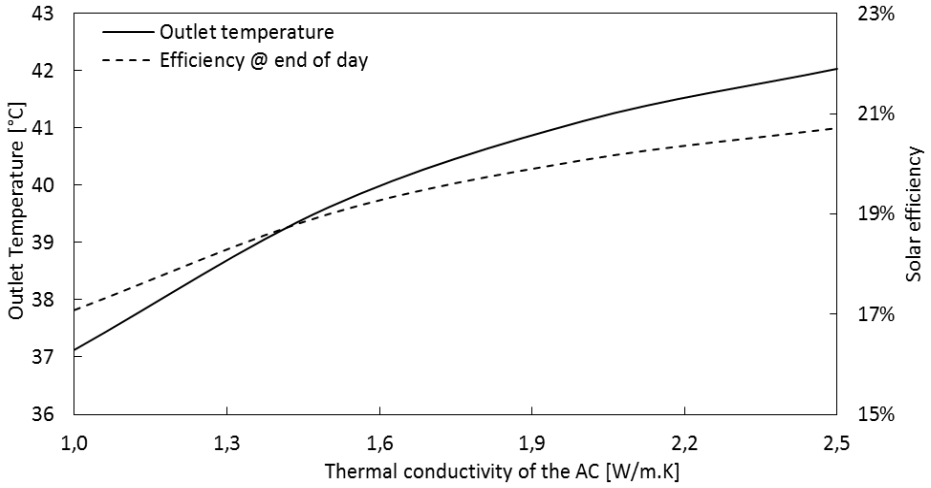

Figure 8: Outlet temperature and solar efficiency as a function of thermal conductivity of the asphalt concrete

Figure 9 presents the outlet temperature of the HEAL as a function of time. The dry-bulb air temperature and solar insolation are projected as well, which clearly shows the latency of the HEAL energy output over the solar insolation. This graph also depicts the

influence of the depth of the pipe. A decrease in energy output due to a larger pipe depth – potentially necessary in case of an increase in traffic loads – can clearly be compensated by a larger thermal conductivity. This highlights the importance of increasing the thermal conductivity.

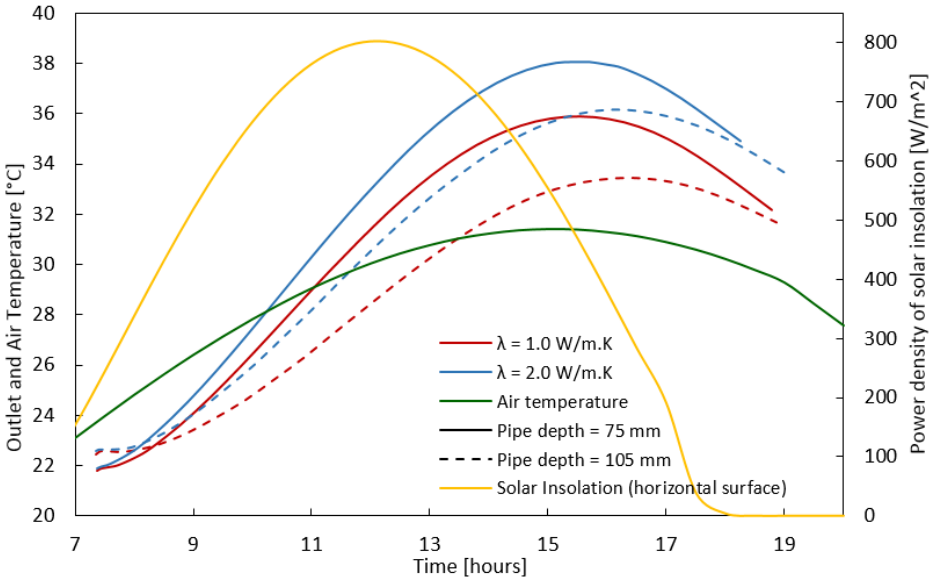

Figure 9: Outlet temperature and power density as a function of time, for different thermal conductivities and pipe depths.

The high solar absorptivity (α) value of asphalt concrete is one of the key reasons why the HEAL is very often preferred in combination with asphalt concrete pavements, rather than cementitious concrete pavement structures. However, when asphalt concrete ages, it becomes lighter in color and the absorptivity decreases. The effect of a lower absorptivity value of the pavement surface has the effect of a lower overall asphalt concrete temperature, including the pavement surface temperature. The influence of the absorptivity on the HEAL has therefore been investigated in this parametric study, as shown in Figure 10.

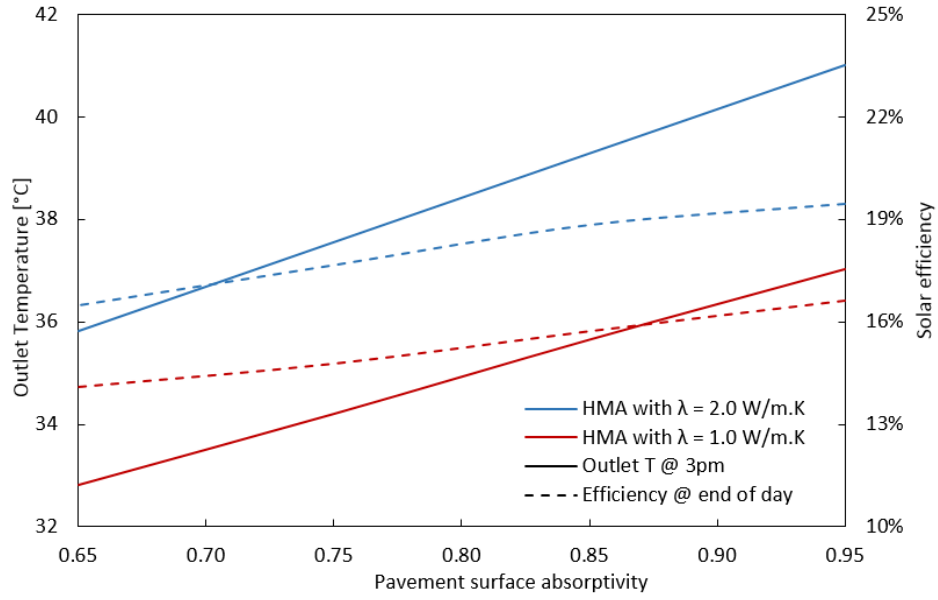

Figure 10: Outlet temperature and solar efficiency as a function of absorptivity of the asphalt concrete surface, for two different thermal conductivities of the AC.

The absorptivity has a linear relationship with the outlet temperature, contrary to the thermal conductivity, which shows a parabolic relationship.

It is clear that the thermal characteristics of the pavement materials have a large influence on the performance of the HEAL. Using granulates with a higher conductivity, for example, can potentially compensate for a wider pipe spacing or a larger pipe depth. Using the developed FE model it will be possible to predict the potential outcome of the HEAL taking into account both the weather, material and geometrical parameters. The next step will be to evaluate all the potential benefits of the HEAL and to determine possible applications taking into account a full cost-benefit analysis or Life Cycle Assessment.

5. CONCLUSIONS

In this paper, a modelling framework is developed using a finite element method to predict the thermal behaviour of a Heat Exchanging Asphalt Layer (HEAL). This model results in a realistic energy output of the HEAL due to the limited amount of simplifications incorporated in the model. The simplifications applied to the model are (i) perfect contact between different materials, (ii) homogenous and isotropic pavement materials, (iii) pure water as working fluid, and (iv) no influence of the fluid flow field by the heat exchange in the HEAL. An experiment was carried out to validate the model. Experimental data and the modelling framework are in good agreement with respect to fluid outlet temperatures and pavement temperatures.
A parametric study on some of the thermal characteristics of the AC has been performed, showing their influence on the system performance. However, a comprehensive study of all geometrical and weather parameters needs to be conducted further using the developed FE model. This way a long term prediction of the energy output of a HEAL can be performed for any location, offering a sound basis for further research regarding the application of this low-temperature heat or potential benefits with regard to the lifetime of the AC.

ACKNOWLEDGEMENTS

The authors of this paper would like to give special thanks to Prof. Dr. Rajib Mallick and Dr. Bao-Liang Chen for the use of their experimental set-up, which was funded by the Massachusetts Technology Collaborative.

REFERENCES

[1] Predicting Maximum Pavement Surface Temperature Using Maximum Air Temperature and Hourly Solar Radiation, T. Kennedy and M. Solaimanian, Transp. Res. Rec., vol. 1417, pp. 1–11, 1993.

[2] Evaluation of the potential of harvesting heat energy from asphalt pavements, R. B. Mallick et al., Int. J. Sustain. Eng., vol. 4, no. 2, pp. 164–171, Jun. 2011.

[3] Harvesting Energy From Asphalt Pavements and Reducing the Heat Island Effect, R. B. Mallick et al., Int. J. Sustain. Eng., vol. 2, no. 3, pp. 214–228, Sep. 2009.

[4] Harvesting Heat Energy From Asphalt Pavements: Development of and Comparison Between Numerical Models and Experiment, R. B. Mallick et al., Int. J. Sustain. Eng., vol. 5, no. 2, pp. 37–41, 2011.

[5] Influence of the Thermophysical Properties of Pavement Materials on the Evolution of Temperature Depth Profiles in Different Climatic Regions, M. R. Hall et al., J. Mater. Civ. Eng., vol. 24, no. 1, pp. 32–47, 2012.

[6] Asphalt Solar Collectors: A Literature Review, V. Bobes-Jesus et al., Appl. Energy, vol. 102, pp. 962–970, Feb. 2013.

[7] Horizontal Concrete Slabs as Passive Solar Collectors, E. Bilgen and M.-A. Richard, Sol. Energy, vol. 72, no. 5, pp. 405–413, May 2002.

[8] Thermal and Hydraulic Analysis of Multilayered Asphalt Pavements as Active Solar Collectors, P. Pascual-Muñoz et al., Appl. Energy, vol. 111, pp. 324–332, Nov. 2013.

[9] Capture Solar Energy and Reduce Heat-Island Effect from Asphalt Pavement, B. L. Chen, PhD thesis, Worcester Polytechnic Institute, 2008.

[10] Laboratory Investigation Into Thermal Response of Asphalt Pavements as Solar Collector by Application of Small-Scale Slabs, W. Shaopeng et al., Appl. Therm. Eng., vol. 31, no. 10, pp. 1582–1587, Jul. 2011.

[11] Parametric analysis of energy harvesting pavements operated by air convection, A. Chiarelli et al., Applied Energy, vol. 154, pp. 951-958, 2015.

[12] Asphalt Pavement Temperature Prediction, M. J. C. Minhoto et al., Road Mater. Pavement Des., vol. 1919, no. 1, pp. 96–110, 2005.

[13] Mathematical Model for Paved Surface Summer and Winter Temperature: Comparison of Calculated and Measured Temperatures, Å. Hermansson, Cold Reg. Sci. Technol., vol. 40, pp. 1–17, Nov. 2004.

[14] Modelling Temperature and Energy Balances within Geothermal Paving Systems, K. Tota-Maharaj et al., Road Mater. Pavement Des., vol. 12, no. 2, pp. 315–344, Jun. 2011.

[15] Modeling Temperature Distribution in Rigid Pavement Slabs: Impact of Air Temperature, Y. Qin and J. E. Hiller, Constr. Build. Mater., vol. 25, no. 9, pp. 3753–3761, Sep. 2011.

[16] Fundamentals of Heat and Mass Transfer, F. P. Incropera et al., Seventh ed., John Wiley & Sons, 2007.

[17] The Relationship Between Relative Humidity and the Dewpoint Temperature in Moist Air: A Simple Conversion and Applications, M. G. Lawrence, Bull. Am. Meteorol. Soc., vol. 86, no. 2, pp. 225–233, Feb. 2005.

[18] A Heat-Transfer Model for Evaluating Frost Action and Temperature-Related Effects in Multilayered Pavement Systems, M. R. Thompson and B. J. Dempsey, Highw. Res. Rec., pp. 39–56, 1970.

[19] Impact of Pavement Thermophysical Properties on Surface Temperatures, J. G. Gui et al., J. Mater. Civ. Eng., vol. 19, no. 8, pp. 683–690, 2007.